Genetic dissection of assortative mating behavior

Richard M. Merrill [1,2,3,*], Pasi Rastas[2], Simon H. Martin[2], Maria C. Melo[3,4], Sarah Barker[2], John Davey[2,5], W. Owen McMillan[3] & Chris D. Jiggins[2]

1 Division of Evolutionary Biology, Ludwig-Maximilians-Universität, München, Germany **2** Department of Zoology, University of Cambridge, Cambridge, UK **3** Smithsonian Tropical Research Institute, Panama City, Panama **4** IST Austria, Klosterburg, Austria **5** Department of Biology, University of York, York, UK

*merrill@bio.lmu.de

Abstract

The evolution of new species is made easier when traits under divergent ecological selection are also mating cues. Such ecological mating cues are now considered more common than previously thought, but we still know little about the genetic changes underlying their evolution, or more generally about the genetic basis for assortative mating behaviors. Both tight physical linkage and the existence of large effect preference loci will strengthen genetic associations between behavioral and ecological barriers, promoting the evolution of assortative mating. The warning patterns of *Heliconius melpomene* and *H. cydno* are under disruptive selection due to increased predation of non-mimetic hybrids, and are used during mate recognition. We carried out a genome-wide quantitative trait locus (QTL) analysis of preference behaviors between these species and showed that divergent male preference has a simple genetic basis. We identify three QTLs that together explain a large proportion (~60%) of the differences in preference behavior observed between the parental species. One of these QTLs is just 1.2 (0-4.8) cM from the major color pattern gene *optix*, and, individually, all three have a large effect on the preference phenotype. Genomic divergence between *H. cydno* and *H. melpomene* is high but broadly heterogenous, and admixture is reduced at the preference-*optix* color pattern locus, but not the other preference QTL. The simple genetic architecture we reveal will facilitate the evolution and maintenance of new species despite on-going gene flow by coupling behavioral and ecological aspects of reproductive isolation.

Introduction

During ecological speciation, reproductive isolation evolves as a result of divergent natural selection [1]. Although ecological barriers can reduce gene flow between divergent populations, speciation normally requires the evolution of assortative mating [1,2]. This is made easier if traits under divergent ecological selection also contribute to assortative mating, as this couples ecological and behavioral barriers [3–6]. Ecologically relevant mating cues (sometimes known as 'magic traits' [2,6]) are now predicted to be widespread in nature [6,7], and the last few years have seen considerable progress in our understanding of their genetic basis. For example, studies have explored the genetic basis of beak shape in Darwin's finches [8], body shape in sticklebacks [9,10], cuticular hydrocarbons in *Drosophila* [11], and wing patterns in *Heliconius* butterflies [12–14]. However, the extent to which these traits contribute to assortative mating depends on the evolution of corresponding preference behaviors, and the underlying genetic architecture.

We still know little about the process by which ecological traits are co-opted as mating cues, and in particular, how matching cues *and* preference behaviors are controlled genetically (but see [15]). Both the substitution of large effect preference alleles, and physical linkage will strengthen linkage disequilibrium ('LD', *i.e.* the non-random association of alleles at different loci [16]) between cue and preference. Strong LD between barrier loci is expected to both maintain and facilitate the evolution of new species in the face of gene flow. This is the result of two key, but related processes. First, LD between barrier loci will result in the coupling of barrier effects, and where these effects coincide the overall barrier to gene flow is increased [4,16]. Second, LD between pre- and post-mating barrier loci will facilitate an increase in premating isolation in response to selection against hybridization (*i.e.*

reinforcement, *sensu* [18]), by transferring the effects of selection from the latter to the former [19].

In central Panama, the butterfly *Heliconius melpomene rosina* is a precise Müllerian mimic of *H. erato* and normally occurs in forest-edge habitats, whereas the closely related species *H. cydno chioneus* mimics *H. sapho* and is more common in closed-forest habitats, although *H. melpomene* and *H. cydno* are often seen flying together (Fig. 1a & b) [20]. Hybrids are viable but occur at very low frequency in the wild (estimated at ~0.1%), consistent with strong assortative mating shown in insectary experiments. Specifically, heterospecific mating was not observed in 50 choice and no-choice trials between Panamanian *H. melpomene* and *H. cydno* ([21,22] ; see also [23]).

The amenability of *Heliconius* color patterns to experimental manipulation has led to the demonstration that color pattern is both under strong disruptive selection due to predation [24], and also that males prefer live females and paper models with the same color pattern as themselves [24]. These results led Servedio and colleagues [6] to conclude that, unlike other putative examples, both criteria for a magic trait have been confirmed with manipulative experiments in *H. melpomene rosina* and *H. cydno chioneus*. Although female preferences undoubtedly contribute to assortative mating [25–27], male preferences act first in these species such that strong observed male discrimination against heterospecific females will have a disproportionate contribution to overall reproductive isolation [28]. As highlighted by Coyne and Orr [29], the order in which reproductive isolation acts influences their relative contribution to overall isolation. In this case, the ordering of behavioral decisions is likely predetermined by their sensory systems: *Heliconius* lack specialized olfactory structures to support long range detection of chemical signals,

103 so are only likely to use these in close proximity, whereas they have very good long-
104 range vision [30]. As such, not only is male preference in *Heliconius* butterflies
105 experimentally more tractable than other components of behavioral isolation, it is also
106 an important barrier to gene flow.

107 Crossing experiments have shown that the shift in mimetic warning pattern
108 between *H. melpomene rosina* and *H. cydno chioneus* is largely controlled by just
109 three major effect loci [31]. Genes underlying these loci have now been identified: the
110 transcription factor *optix* controls red patterns [12], the *WntA* gene controls forewing
111 band shape [13] and yellow patterns map to the gene *cortex* [14]. In addition, a
112 further locus, *K*, segregates in crosses between *H. melpomene rosina* and *H. cydno*
113 *chioneus* with more minor effect [31]. Further modularity occurs within these loci. For
114 example, different regulatory elements of *optix* each result in distinct red pattern
115 elements [32]. The modular nature of individual color pattern loci and their
116 functionally sufficient enhancers means that they can be combined to produce
117 considerable phenotypic diversity [32,33]. These loci are large-effect 'speciation
118 genes', in that they control traits that generate strong reproductive isolation [34].

119 Two of these color pattern loci, *optix* and *K,* have previously been associated
120 with *Heliconius* courtship behaviors [25,35,36]; however, these studies do not provide
121 evidence for tight physical linkage (<20cM) between warning pattern and preference
122 loci. Our own previous study tested for an association between Mendelian color
123 pattern loci and preference behaviors [25], but did not correct for the segregation of
124 alleles across the genome, so that reported levels of support are likely inflated [37];
125 and an earlier study of the parapatric *taxa H.* cydno *and H. pachinus* [35] is limited by
126 small sample size [37]. Regardless of the level of statistical support for preference
127 QTL, these studies both lack the resolution to demonstrate the degree of tight

128 physical linkage between loci contributing to reproductive isolation that would be
129 expected to aid speciation. Perhaps the best evidence comes a study of wild *H.*
130 *cydno alithea* [36]. This population is polymorphic for a yellow or white forewing (due
131 to the segregation of alleles at the *K* locus), and males with a yellow forewing prefer
132 yellow females. These results are important because they suggest a key component
133 of speciation: Specifically, coupling between potential behavioral and ecological
134 barriers. However, because they rely on segregation within a wild population, rather
135 than laboratory crosses, it is not possible to distinguish physical linkage from genetic
136 associations between cue and preference alleles due to non-random mating. The
137 extent to which warning pattern and behavioral loci are physically linked in
138 *Heliconius*, as well as the existence of major preference loci elsewhere in the
139 genome remains unknown. To address this, and to complement our extensive
140 knowledge of the genetics of their color pattern cues, here we use a genome-wide
141 quantitative trait locus (QTL) approach to explore the genetics of male preference
142 behaviors between the sympatric species *H. melpomene rosina* and *H. cydno*
143 *chioneus*.
144

145 **Results**

146 We studied male mating preference among F1 and backcross hybrid families
147 between *H. melpomene rosina* and *H. cydno chioneus*, in standardized choice trials
148 [25,38] (Figs. 1 and S1). We introduced individual males into an experimental cage
149 and recorded courtship directed towards two virgin females, one of each species. In
150 total, we collected data from 1347 behavioral trials, across 292 individuals. Multiple
151 trials were performed for each backcross male, from which we determined the
152 relative courtship time directed towards *H. melpomene* and *H. cydno* females.

153 **Figure 1. Divergence in warning pattern cue and corresponding preference in sympatric**
154 ***Heliconius* butterflies.** A, Wing pattern phenotypes of: top, *Heliconius cydno chioneus* (left), *H.*
155 *melpomene rosina* (right) their non-mimetic first generation hybrid (center), and bottom, their sympatric
156 co-mimics *H. sapho sapho* (left) and *H. erato demophoon* (right). B, Distribution of *H. cydno* (blue) and
157 *H. melpomene* (orange). Individuals were collected, and experiments performed in Panama (black
158 circle), where the two species co-occur in Central and northern South America. **C**, Proportion of
159 courtships directed towards *H. melpomene* (as opposed to *H. cydno*) females for *H. cydno* (CYD), *H.*
160 *melpomene* (MEL), their F1 and backcross hybrids to *H. cydno* (BC) and *H. melpomene* (BM). Values
161 in parentheses indicate total number of individuals with behavioral data. Solid colored boxes represent
162 expected average genome contribution of each generation. Note that a further 11 BC individuals were
163 tested but performed no courtship behaviors.

164

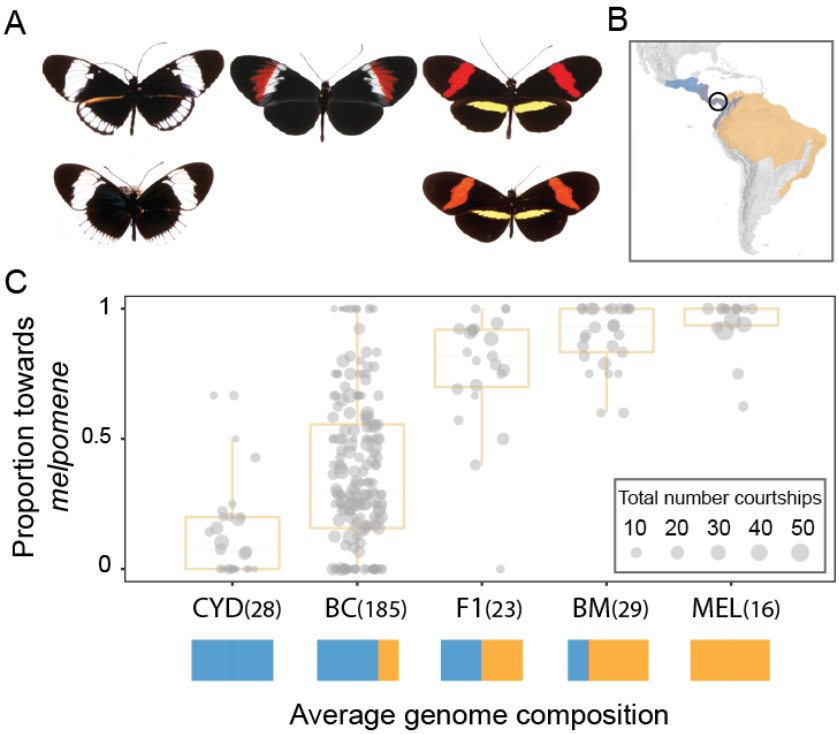

165

166

167

168 **Three loci contribute to species differences in preference behavior.** As reported
169 previously [25], F1 males have a strong preference for the red *H. melpomene*
170 females, and little segregation in mate preference is observed among the backcross
171 to *melpomene* (and whose mean preference does not differ significantly from that of

172 **Figure 2. QTL analysis of variation in mate preference.** A, QTLs for relative time males court *H.*
173 *melpomene* (as opposed to *H. cydno*) females on chromosomes 1, 17 and 18 (n = 139). Scale on right
174 axis depicts genome-wide significance, determined through permutation, corresponding to the LOD
175 score as shown on the left axis. Dotted red line represents log odds ratio (LOD) significance threshold
176 (genome-wide alpha = 0.05, LOD = 2.99). Dashes indicate position of genetic markers (SNPs) and red
177 arrows indicate the position of the max LOD score for each QTL (used in B). Vertical blue lines
178 represent the position of major color pattern loci, and their phenotypic effects. Note that the *K* locus
179 only has limited phenotypic effects in crosses between *H. cydno chioneus* and *H. melpomene rosina*,
180 but is responsible for the switch from yellow to white color pattern elements between other taxa within
181 the *melpomene-cydno* clade. B, Proportion of time males court *H. melpomene* (as opposed to *H.*
182 *cydno*) females for each of the two genotypes for respective QTLs (homozygous = CYD: CYD, and
183 heterozygous = CYD:MEL). Error bars represent 95% confidence intervals. Lower dashed blue and
184 upper orange bars represent mean phenotypes measured in *H. cydno* and *H. melpomene,*
185 respectively. Circle size depicts total number of 'courtship minutes' for each male. Vertical black bars
186 indicate the percentage of the difference measured in the parental species explained.

187

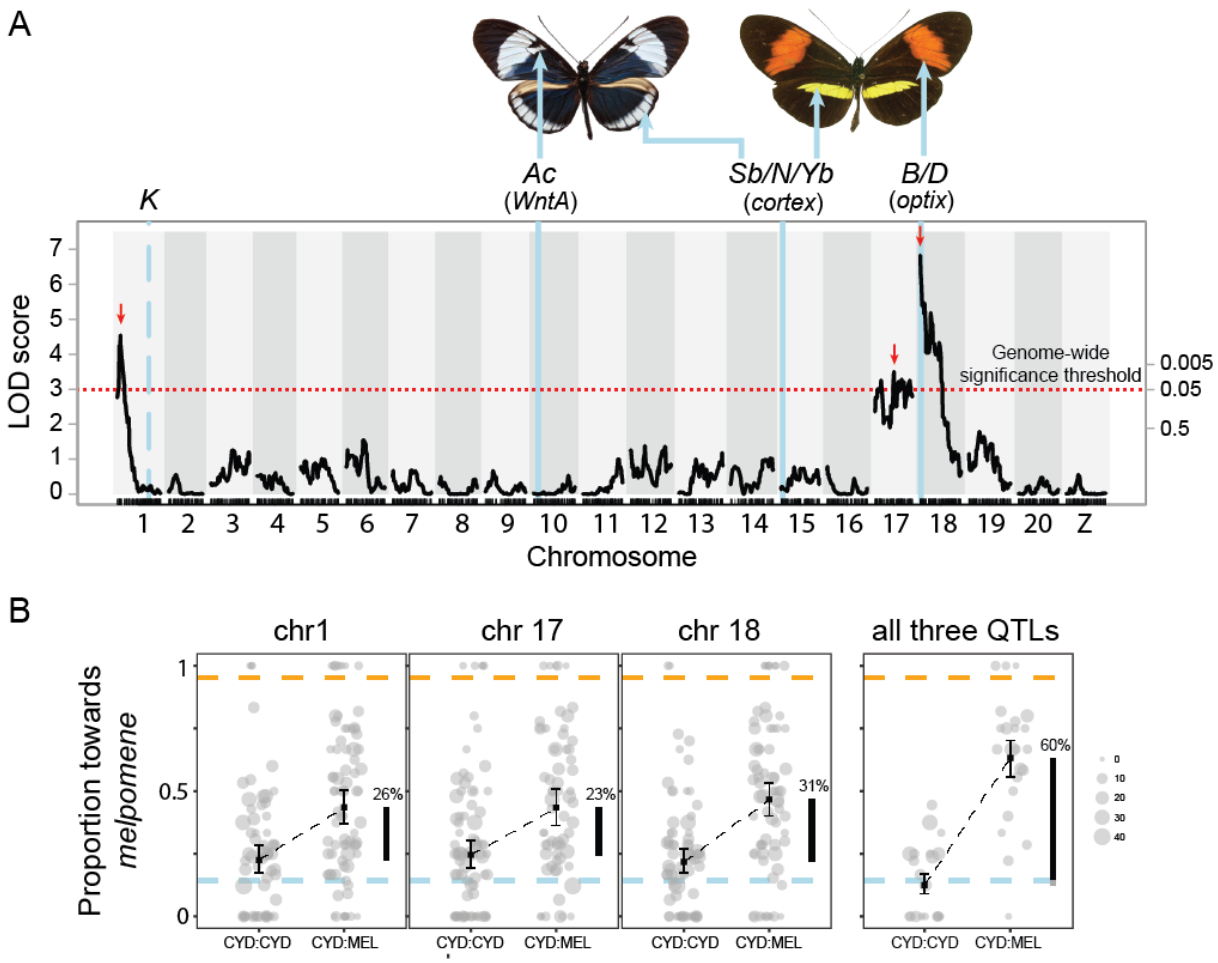

188

189 pure *H. melpomene* males: 2ΔlnL = 1.33, *d.f.* = 1, *P* > 0.2), implying that *melpomene*
190 mate preference alleles are dominant. In contrast, courtship behavior segregates
191 among *H. cydno* backcross males, permitting analysis of the genetic basis for this
192 mating behavior (Fig. 1C). Consequently, all subsequent analyses were performed
193 on backcross to *cydno* males. We used a genome-wide quantitative trait locus (QTL)
194 mapping approach to identify the genomic regions underlying divergence in mate
195 attraction. Linkage maps were constructed from genotype data of 331 backcross-to-
196 cydno individuals and their associated parents [39], including 146 individual males for
197 which we had recorded attraction behaviors.

198 We identified three unlinked QTLs on chromosomes 1, 17 and 18 associated
199 with variation in the relative amount of time males spent courting red *H. melpomene*
200 and white *H. cydno* females (Fig. 2A). Of these, one is tightly linked to the *optix* locus
201 on chromosome 18, which controls the presence/absence of a red forewing band.
202 Specifically, the QTL peak for the behavioral QTL on chromosome 18 (at 0cM) is just
203 1.2cM from *optix.* The associated 1.5-LOD support interval is between 0 and 6.0cM,
204 suggesting that the true location of the QTL is no more than 4.8cM from the *optix*
205 coding region (whose genetic position is at 1.2cM) (Fig. 3); however, given that the
206 peak support (i.*e.* highest LOD score) for our behavioral QTL is at 0cm and that this
207 rapidly drops off, physical linkage between wing patterning cue and preference loci is
208 likely much tighter than a strict 1.5-LOD interval might suggest. In contrast, the QTL
209 on chromosome 1 is at least 30cM from the gene *wingless*, which although unlikely to
210 be a color pattern gene itself has previously been associated with the *K* wing pattern
211 locus between taxa within the *cydno* clade [35]. No known wing pattern loci reside on
212 chromosome 17 and this chromosome does not explain any of the pattern variation
213 segregating in our BC pedigrees (Merrill, unpublished data).

214 **Figure 3. Genetic and physical positions of behavioral QTL and the warning pattern loci, and**
215 **localized levels of admixture (f_d).** Vertical blue lines represent the position of major color pattern loci
216 and orange lines represent the position of peak LOD score for each behavioral QTL. Gray boxes
217 indicate the 1.5-LOD support interval for each QTL. Top panel: Dashes along the x-axis indicate
218 position of genetic markers (SNPs). Bottom panel: Blue points represent f_d values for 100kb
219 windows. f_d was measured between *H. melpomene rosina* and *H. cydno chioneus* individuals from
220 populations samples in Panama; *H. melpomene melpomene* from French Guiana, which is allopatric
221 with respect to *H. cydno*, was the 'control' population.
222

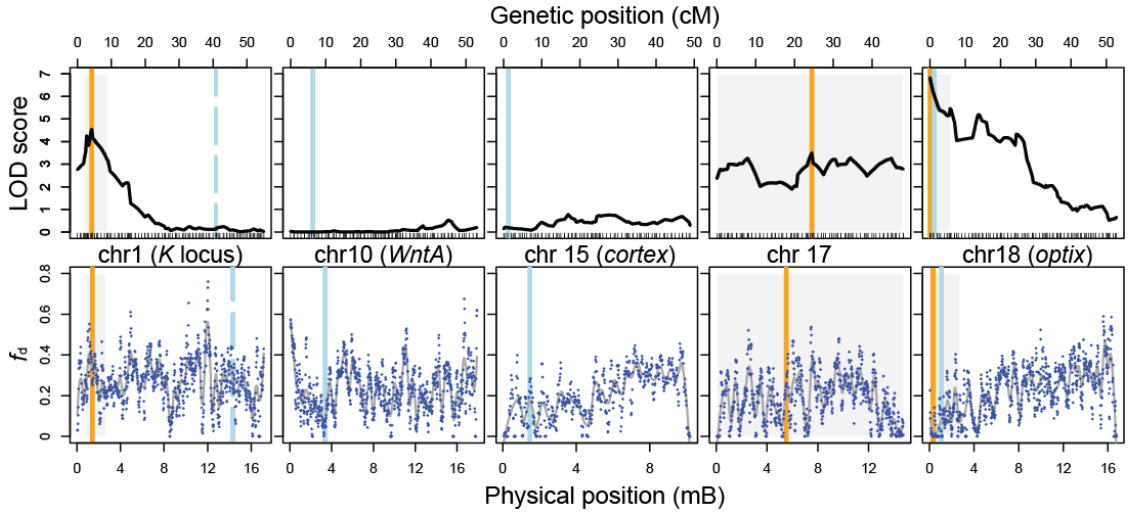

223
224

225

226 Modeling supports additive effects of all three detected loci (Table 1), and in
227 our mapping population these three QTLs together explain ~60% of the difference in
228 male preference behavior between the parental species (Fig. 2B). Given the sample
229 sizes feasible in *Heliconius*, our analysis lacks the power to resolve smaller effect
230 QTLs. We also found no evidence of pairwise interactions between individual QTLs
231 in our model of relative courtship time, which again is unsurprising given achievable
232 sample sizes. However, genome scans considering individuals with alternative
233 genotypes at the QTL on chromosome 18 separately revealed a significant QTL on
234 chromosome 17 (LOD = 3.52, *P*=0.016) for heterozygous (i.e. LG18@0cM =

235 CYD:MEL), but not for homozygous (i.e. LG18@0cM = CYD:CYD) males (Fig. S2),
236 though this result is not supported by non-parametric interval mapping (LOD = 2.4,
237 *P*=0.132). Nevertheless, these results perhaps suggest that alleles on chromosomes
238 17 and 18, or the specific behaviors they influence, may interact.
239
240 **Table 1. Individual and combined QTLs for differences in relative courtship time.**

Chromosome	Position (cM)	LOD score	Δ*p*LOD*a*	2ΔlnL	*P*
1	4.2 (2-9.1)	4.54	-1.04	18.54	<0.001
17	24.4 (0-48.3)	3.50	-1.03	18.50	<0.001
18	0 (0-6)	6.83	-3.87	31.60	<0.001
1+17+18	**–**	**14.90**	**(5.93)**	**–**	**–**

Position in cM (1.5 LOD interval); LOD score, log odds ratio; Δ*p*LOD*a*, penalized LOD score, change in penalized LOD score compared to the full (best supported) model incorporating all three putative QTLs (in bold); 2ΔlnL & *P* values compare the full model to reduced models in which individual QTLs were eliminated; *n* = 139.

241
242 **Preference QTL are of large effect.** Individually, the measured effect of each of the
243 three QTLs we identified was large, explaining between 23 and 31% of the difference
244 between males of two parental species (Fig. 2B). However, in studies with relatively
245 small sample sizes such as ours (*n* = 139), estimated effects of QTL are routinely
246 over-estimated (a phenomenon known as the "Beavis effect", after [40]). This is
247 because effect sizes are determined only after significance has been determined,
248 and QTL with artificially high effect sizes – due to variation in sampling – are more
249 likely to achieve 'significance'.
250 To determine the extent to which the effects of our QTL may be over-
251 estimated, we simulated QTL across a range of effect sizes, and compared the
252 distribution of measured effects for all simulations to those which would be significant
253 in our analysis (Fig. S3). Our simulations suggest that the reported effects of our QTL
254 are not greatly over-estimated. We first considered what proportion of 'significant'
255 simulations would be smaller than our empirically measured effects (Fig. 4A). This

256 suggests that the true effect sizes of our QTL are likely to be large, with somewhat
257 less support for the QTL on chromosome 17. A highly conservative threshold of 95%
258 would suggest that the QTL on chromosome 1 and 18 explain at least 10% and 20%
259 of the difference in behavior between the parental species, respectively. Adopting the
260 median values, our simulations would suggest true effects of 25%, 15% and 30%, or
261 greater, for the QTL on chromosomes 1, 17 and 18, respectively. Given simulated
262 effect sizes similar to those measured empirically, there was little bias among
263 simulation runs that achieved the genome-wide significance threshold (Fig. S3). This
264 suggests that the true effect sizes of our QTL are likely to be large, with somewhat
265 less support for the QTL on chromosome 17.

266 Although our simulations suggest the effects we have measured are
267 reasonable, ideally we would estimate effect sizes from a population of individuals
268 that were not used to determine significance. In evolutionary biology, follow-up
269 experiments such as this are uncommon; collecting phenotypic data across a large
270 number of hybrid individuals is often a considerable undertaking, and this is similarly
271 true for *Heliconius* behaviors. Nevertheless, we were able to follow-up our results for
272 the QTL on chromosome 18, using a sample of a further 35 backcross males for
273 which preference behavior was measured, but for which we were unable to generate
274 genotype data (and so were not included in our initial QTL analysis). As reported
275 above, the QTL peak (at 0cM) on chromosome 18 is in very tight linkage with the
276 *optix* color pattern locus (at 1.2cM), which controls the presence and absence of the
277 red forewing band. Presence of the red forewing band is dominant over its absence,
278 so that segregation of the red forewing band can be used to perfectly infer genotype
279 at the *optix* locus, even without sequence data. This analysis supports our previous
280 result that the QTL on linkage group 18 is of large effect (Fig. 4B): among these 35

281 hybrid males, the *optix* locus explains 27% of the difference in behavior between the
282 parental species (*c.f.* 31% for the larger mapping population).

283

284 **Figure 4. QTL effects in consideration of the to the Beavis effect.** A, Proportion of 'significant'
285 simulations that would be smaller than our empirically measured effects, for preference QTL on
286 chromosome 1 (blue), chromosome 17 (black), and chromosome 18 (orange). 10000 simulations were
287 run for effect sizes corresponding to between 5 and 40% of the difference in male preference behavior
288 between the parental species. In each case the distribution of sample effect sizes was determined for
289 those simulations that reached the genome-wide significance threshold determined through
290 permutation (Fig. 2). B, Proportion of time males court *H. melpomene* (as opposed to *H. cydno*)
291 females for each of the two genotypes for white (homozygous = CYD:CYD) and red (heterozygous =
292 CYD:MEL) hybrid males for which we were unable to generate RAD data (and so which were not
293 included in our initial QTL analysis). Error bars represent 95% confidence intervals. Lower dashed
294 blue and upper orange bars represent mean phenotypes measured in *H. cydno* and *H. melpomene,*
295 respectively. Circle size depicts total number of 'courtship minutes' for each male. Vertical black bars
296 indicate the percentage of the difference measured in the parental species explained.

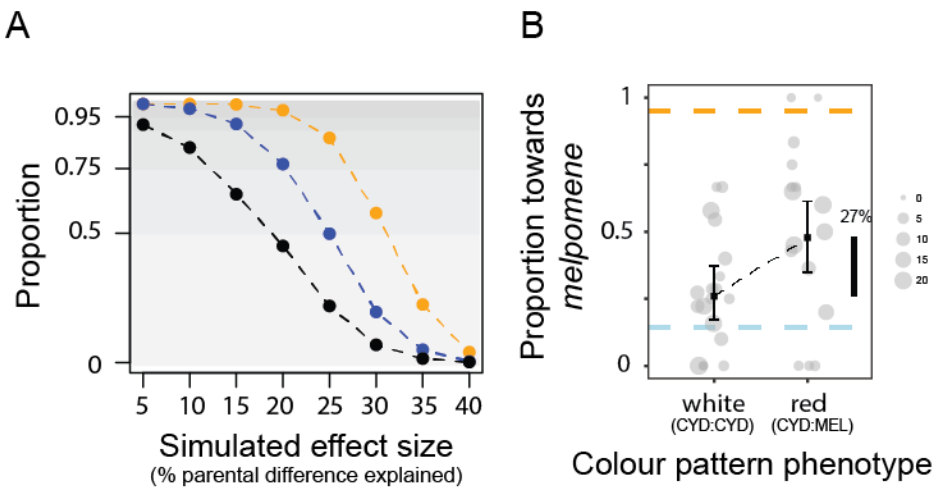

297

298

299 **Admixture is reduced at the preference-color pattern locus on chromosome 18.**
300 To consider the effects of major color pattern cue and preference loci on localized
301 gene flow across the genome we used the summary statistic f_d to quantify admixture
302 between *H. cydno chioneus* and *H. melpomene rosina* (Fig. 3 and S4). f_d is based on
303 the so-called ABBA-BABA test and provides a normalized measure that

304 approximates the proportional effective migration rate (*i.e.* $f_d = 0$, implies no localized
305 migration of alleles, whereas $f_d = 1$, implies complete localized migration of alleles)
306 [41,42]. At the physical location of our behavioral QTL on chromosome 18, which is
307 in tight linkage with the *optix* color pattern locus, there is a substantial reduction in
308 admixture across a ~1 megabase region. At our other two QTLs, reduced f_d values
309 (<0.1) are observed for individual 100kb windows associated with all behavioral QTL
310 (specifically, within the 1.5-LOD intervals); but, this is true for many sites across the
311 genome. In addition to mating behavior these two species differ among a number of
312 other behavioral and ecological axes and genomic divergence is highly
313 heterogenous.
314
315 **Different preference QTL affect different aspects of behavior.** The male
316 preference QTLs we have identified may influence differences in male attraction
317 towards red *H. melpomene* females, or white *H. cydno* females, or towards both
318 female types. To further explore the influence of segregating alleles at these loci we
319 considered the influence of all three QTLs on courtships directed towards each
320 female type separately (Fig. 5). We have already robustly established a significant
321 effect of these loci on variation in the relative amount of time males spent courting
322 each female type (see Fig. 2A). Consequently, although we corrected for multiple
323 testing arising from considering three QTL across the two data sets [37], in these
324 *post-hoc* analyses we did not account for multiple segregating loci across the entire
325 genome (in contrast to the results reported above). This greatly increases our power
326 to detect any influence of the QTLs on attraction towards the two species individually,
327 but also increases the likelihood of false positives. The QTL on chromosome 1
328 influenced the number of courtships directed towards *H. cydno* females ($F_{1,145}$ =

329 10.85, $P < 0.01$), but had no significant effect on how males behaved towards *H.*
330 *melpomene* females ($F_{1,145} = 1.35$, $P > 0.2$). In contrast, the QTL on chromosome 17
331 influenced the degree of courtship directed towards *H. melpomene* ($F_{1,145} = 10.08$, P
332 $= 0.011$), but not *H. cydno* females ($F_{1,145} = 0.41$, $P > 0.2$). Similarly, the QTL on
333 chromosome 18 had a significant effect on courtships directed towards *H.*
334 *melpomene* ($F_{1,145} = 9.93$, $P = 0.012$) females (though we note that prior to Bonferroni
335 correction there is also some support for an effect on courtships directed towards *H.*
336 *cydno* females: $F_{1,145} = 6.56$, $P = 0.01$).
337
338 **Figure 5. Different QTL affect different aspects of behavior.** The QTL on chromosome 1 influences
339 courtship towards *H. cydno,* but not *H. melpomene* females. The opposite is the case for the QTLs on
340 chromosomes 17 and 18, where there is little evidence that either QTL influence courtships directed
341 towards *H. cydno* females. Data presented are for number courtship events corrected by the total
342 number of trials. Blue circles and boxplots represent data for individuals homozygous at each QTL (i.e.
343 CYD:CYD), orange circles and boxplots represent data for individuals heterozygous at each QTL (i.e.
344 CYD:MEL)

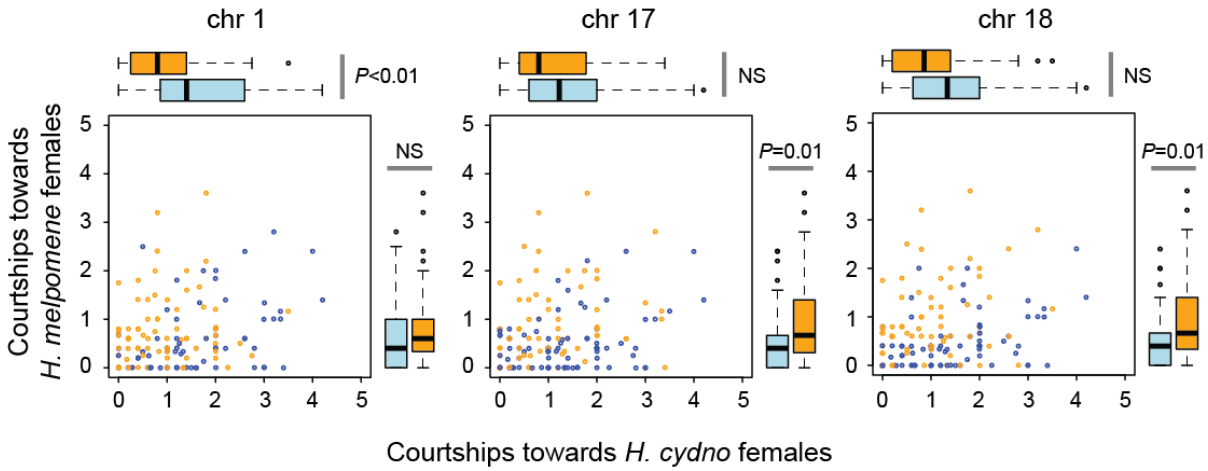

345
346

Discussion

348 Here, we reveal a genetic architecture that will strengthen genetic associations (*i.e.*
349 LD) between key components of reproductive isolation, and so facilitate ecological
350 speciation in the face of gene flow. Specifically, we demonstrate that just three QTLs

351 are largely responsible for an important component of behavioral isolation between
352 two sympatric species of *Heliconius* butterfly. One of these resides only 1.2 (0-4.8)
353 cM from a major color pattern gene. Our results also suggest that all three preference
354 loci are of large phenotypic effect. Because LD between cue and preference loci will
355 arise as a natural consequence of mating preferences [43], these large effect
356 preference loci will further increase LD between ecological and behavioral
357 components of reproductive isolation. Additional smaller effect loci undoubtedly also
358 contribute to variation in male preference, which we would be unlikely to detect
359 without very large sample sizes (a caveat shared with many QTL studies of
360 ecologically relevant behaviors e.g. [15,44,45]). Regardless, our results suggest that
361 during speciation, divergence between populations in both mating cue and the
362 corresponding preference behaviors can have a surprisingly simple genetic
363 architecture.

364 By ensuring robust genetic associations between components of reproductive
365 isolation, physical linkage between loci for traits influencing pre- and post-mating
366 isolation is expected to facilitate speciation with gene flow [19]. Two of the behavioral
367 QTL we have identified are situated on chromosomes with major color pattern loci
368 (chromosome 1 includes the *K* locus, and chromosome 18 includes the *optix* locus).
369 Both *optix* and the *K* locus have previously been associated with variation in
370 *Heliconius* courtship behaviors [25,35,36]. Nevertheless, we have not previously
371 been able to robustly estimate the position of QTLs along the chromosome. The QTL
372 we identify on chromosome 1 is not tightly linked to the *K* locus. It remains to be seen
373 whether this QTL underlies the association between male preference behavior and
374 the *K* locus phenotype (a shift between white and yellow color pattern elements)
375 previously observed in crosses between *H. cydno* and *H. pachinus* [35], and within a

376 polymorphic population of *H. cydno* [36]. (Although the *K* locus phenotype
377 segregating in crosses between *H. cydno* and *H. melpomene* [39] has not been
378 mapped, it is very likely that it is the same locus as that observed in *H. cydno* and *H.*
379 *pachinus*). In contrast, our results reveal that the QTL for male attraction on
380 chromosome 18 is tightly linked to the *optix* locus, which controls presence/absence
381 of a red forewing. The mechanistic basis for linkage of trait and preference loci
382 remains unclear. There is no evidence for an inversion at this locus [39]; it also
383 seems unlikely that the same mutations control both wing pattern and the
384 corresponding attraction behavior. However, *optix* is known to function during eye
385 and neural development in *Drosophila* [46], and is expressed in the optic lobe and
386 medulla of pupal *Heliconius* [47], so it is plausible – if unlikely [48] – that the two traits
387 could be controlled by different regulatory elements of the same gene.
388 Our work joins a small collection of studies in animals where physical linkage
389 is reported to couple loci contributing to preference behaviors and ecological barriers
390 [15,25,35,36,49], as predicted by Felsenstein [19]; and more broadly between loci for
391 cue and preference between incipient species [50–55]. In a seminal study,
392 published almost 20 years ago, Hawthorn and Via [49], showed that QTL for
393 preference and performance for different host plants co-segregate in pea aphids.
394 These insects mate on their host providing a rapid path to speciation. The resolution
395 of molecular markers available at the time allowed linkage to be confirmed to no
396 more than ~10cM, but even this could substantially impede the break-down of LD:
397 whereas LD between unlinked loci declines by 50% in one generation of random
398 mating, LD between two loci that are 10cM apart would decline by only ~9% per
399 generation (cyclical parthenogenesis would further reduce recombination in these
400 aphid species). Extending the same logic to our results, LD between the preference

401 locus and *optix* on chromosome 18 would be expected to decline by 1.2 (0-4.6) %
402 per generation (Fig S5), assuming random mating. However, alleles at the behavioral
403 locus result in a preference for the trait controlled by *optix:* LD will be further
404 maintained by non-random mating because warning pattern is a magic trait. As such
405 LD is likely to decline much more slowly than this simple model would suggest.
406 More recently, Bay and colleagues [15] have reported widespread physical
407 linkage between loci for divergent mate choice and ecological phenotypes in benthic
408 and limnetic populations of three-spine sticklebacks. Two lines evidence support this.
409 First, individual QTLs for mate choice and morphology map to chromosome 14.
410 Second, a polygenic QTL model predicting hybrid position along the benthic-limnetic
411 morphological axis, generated by a previous study [10], explains a significant
412 proportion of variance in mate choice, consistent with physical linkage of ecological
413 and mate choice loci. Our results complement this previous work by explicitly
414 demonstrating tight linkage between assortative mating and ecological traits. In
415 addition, our study shows a much simpler genetic architecture, which should further
416 facilitate the maintenance of LD between traits and which is predicted to facilitate
417 speciation [2].
418 When mate choice is based on a preference for divergent ecological traits, this
419 will inevitably couple ecological and behavioral components of reproductive isolation.
420 Furthermore, the strength of LD generated will be proportional to the strength of the
421 mating preference, so a genetic architecture with large-effect loci controlling
422 assortative mating will generate stronger LD than a more polygenic architecture. Both
423 our simulations and replication analysis support the existence of large effect QTLs
424 controlling an important interspecific difference in preference behavior. Even if we
425 adopt an especially cautious approach, the QTLs on chromosomes 1 and 18 would

426 explain *at least* 10% and 20% of the difference in male preference behavior,
427 respectively. However, our follow-up analysis, exploiting individuals that were not
428 used to determine significance (thereby evading the Beavis effect), suggests that
429 these estimates are overly conservative; these data explicitly reinforce our initial
430 estimate for the QTL on chromosome 18, which explains ~30% of the difference
431 between parents. One potential caveat is that the position of the putative QTL and
432 that of *optix* are not the same, but 1.2cM apart; however, any recombination between
433 these loci in the individuals tested will be rare (we expect just 0.42 recombination
434 events between these two loci across 35 individuals), and likely has very limited
435 impact on our estimates of effect size.

436 We observed a dramatic reduction in admixture (estimated using f_d) at the
437 proximal end of chromosome 18, and specifically on the distal side of *optix* coincident
438 with our QTL. It is tempting to ascribe this to the combined effects of the major
439 preference locus we have identified and the color pattern gene *optix.* However, in the
440 populations studied here, the phenotypic effect of *optix* is more striking than the other
441 color pattern loci, and selection against introgression is likely be stronger at this
442 locus. As a result, tight linkage with *optix* makes it impossible to determine any
443 effects of the preference locus alone. Similarly, it is difficult to infer a signal of
444 reduced admixture due to the behavioral QTLs on chromosomes 1 and 17. Levels of
445 F_{st} are high across the genome between *H. cydno* and *H. melpomene* and patterns of
446 admixture across the genome suggest widespread selection against introgression
447 [42]. At this point, the patterns of divergence between *H. cydno* and *H. melpomene*
448 are so heterogenous, it is difficult to disentangle the many processes that could be
449 driving reduced admixture.

450 A general caveat of our results, alongside other studies of the genetics of
451 assortative mating in *Heliconius* [35,36] and elsewhere (e.g. [15,56]), is that it is hard
452 to distinguish between loci affecting preference behaviors *per se*, from other traits
453 that influence the behavior of the opposite sex. Here, we measured the time
454 *Heliconius* males spend courting a particular female, which may depend not only on
455 male attraction, but also on the female's response to male behavior (and in turn the
456 male's response to the female's behavior). Recent work suggests that *H. cydno*
457 females respond differently to *H. pachinus* than conspecifics males [27]. Although
458 there is currently no evidence that female *Heliconius* use color pattern as an
459 interspecific mating (or rejection) cue (but see [57]), it is not inconceivable, and this
460 could perhaps account for the apparent linkage between male interest and forewing
461 color observed in our study and elsewhere [35,36]. In addition, it is possible that
462 either of these QTLs we identified might influence male pheromones, which has been
463 shown to influence female acceptance behaviors within *H. melpomene* [58].
464 Nevertheless, using the same hybrids as studied here, we previously demonstrated
465 that individuals that have inherited the red band allele from *H. melpomene* are more
466 likely to court artificial females with the red *melpomene* pattern, implying that the QTL
467 on chromosome 18, at least, influences male response to a visual cue [25].
468 Regardless of the exact proximate mechanisms involved, the QTLs we identify here
469 influence an important component of male assortative mating behavior.
470 Overall, the scenario we describe reflects one that modeling broadly predicts
471 will generate a strong overall barrier to gene flow through reinforcement [4]:
472 Specifically, the effects of barrier loci on prezygotic isolation are strong,
473 recombination between pre- and post-mating isolation barrier loci is reduced, and
474 hybridization imposes high costs. Indeed, experimental evidence shows that non-

475 mimetic hybrids between *H. melpomene* and *H. cydno* suffer not only increased
476 predation [24], but also reduced mating success [22] and fertility [59]. In addition,
477 males make a considerable reproductive investment by donating a nutrient-rich
478 spermatophore during mating [60,61], so indirect selection against poorly adapted
479 hybrids could strengthen divergent male preferences. Consistent with a role of
480 reinforcement, *H. melpomene* males from French Guiana, outside the range of *H.*
481 *cydno*, are less choosy than males from Panama, where the species co-occur and
482 are known to occasionally hybridize [21]; and similar patterns of reproductive
483 character displacement have been observed elsewhere in the *melpomene-cydno*
484 clade [62].

485 Reinforcement is further promoted when indirect selection, resulting from
486 coupling of prezygotic and postzygotic barrier effects, is supplemented by direct
487 selection [4,63]. In *Heliconius,* divergence in male preferences is likely initiated by
488 divergence in wing pattern, and male preferences are observed between populations
489 with few opportunities for hybridization e.g. [64]. Female re-mating is a rare event
490 [65], and males must compete to find virgin females within a visually complex
491 environment [26]. Divergence in female (and male) wing patterns is driven primarily
492 by strong selection for mimicry, and is likely to impose divergent sexual selection on
493 male preferences to improve their ability to find receptive females. This is similar to
494 examples of assortative mating driven by sensory drive, such as in cichlid fishes [66],
495 but it is perhaps less well appreciated that morphological traits under ecological
496 selection (such as *Heliconius* wing patterns) might impose divergent sexual selection
497 on male preferences in a similar fashion.

498 In addition to a simple genetic architecture, different QTLs appear to control
499 different aspects of preference behavior. Our *post-hoc* analyses suggest that

500 differences associated with QTL1 and QTL17 in the relative amount of time spent
501 courting each female type are driven by differences in attraction to either *H. cydno* or
502 *H. melpomene*, respectively, rather than both species. QTL18 also seems to
503 influence attraction to *H. melpomene* much more strongly than to *H. cydno* females.
504 This genetic modularity, where discrete, independently segregating loci appear to
505 affect different aspects of behavior, may facilitate evolutionary change and innovation
506 by providing a route for rapid evolution of novel behavioral phenotypes [44,67]. In
507 *Heliconius*, this might allow different aspects of mating behavior to evolve
508 independently. It might also allow novel composite behavioral preferences to arise
509 through hybridization and recombination. There is some evidence that this has
510 occurred during hybrid speciation in *Heliconius*. The wing pattern of the hybrid
511 species *H. heurippa* includes both red and yellow pattern elements, which are
512 believed to have originated from the putative parental species *H. melpomene* and *H.*
513 *cydno,* respectively (local Colombian races of *H. cydno* have a yellow, as opposed to
514 white, forewing band) [23]. Not only do *H. heurippa* males prefer this combined
515 pattern over the 'pure' red or yellow patterns of *H. melpomene* and *H. cydno* [23], but
516 'recreated *H. heurippa*', obtained in first generation backcrosses between *H.*
517 *melpomene* and *H. cydno*, prefer the pattern of *H. heurippa* over that of the two
518 putative parents [68]. This is consistent with a hypothesis in which introgression and
519 subsequent recombination of preference alleles are responsible for novel behavioral
520 phenotypes, although further work would be needed to confirm this.
521 In conclusion, the genetic architecture we demonstrate here will promote the
522 evolution of behavioral isolation by strengthening genetic associations between cue
523 and preference. Disassociation of alleles at loci that are physically close on the
524 chromosome is slower compared to that between alleles at more distant loci (due to

525 reduced crossing over), or at loci on different chromosomes. Similarly, the
526 substitution of large effect alleles will also increase linkage disequilibrium between
527 cue and preference, even if they are not physically linked, because preference alleles
528 of larger effect will more often find themselves in the same genome as alleles for the
529 corresponding cue, compared to preference alleles with smaller effects. We cannot
530 currently distinguish whether preference QTL result from single adaptive mutations,
531 or represent multiple functional loci that have built up during the course of speciation.
532 Nevertheless, the genetic basis of *Heliconius* mate preferences is remarkably similar
533 to that for differences in the wing pattern cue. Differences in individual color pattern
534 elements probably do involve multiple, sequential mutations (which target the same
535 gene(s)), but 'ready-made' alleles of large phenotypic effect can be brought together
536 in new combinations through adaptive introgression. The existence of large effect
537 preference loci, potentially influencing different aspects of behavior, could similarly
538 facilitate the origin of novel phenotypes through introgression, and further facilitate
539 rapid speciation.
540

541 **Methods**

542 **Butterfly collection, rearing and crossing design**. All butterfly rearing, genetic
543 crosses and behavioral experiments were conducted at the Smithsonian Tropical
544 Research Institute in Panama between August 2007 and August 2009.
545 We collected wild *Heliconius cydno chioneus* and *Heliconius melpomene rosina* from
546 Gamboa (9°7.4'N, 79°42.2' W, elevation 60 m) and the nearby Soberania National
547 Park, Panama. These were used to establish stocks maintained in insectaries in
548 Gamboa, which were further supplemented with wild individuals throughout the
549 experimental period. We established interspecific crosses by mating wild caught *H.*

550 *melpomene* males to *H. cydno* females from our stock population. In interspecific
551 crosses between *Heliconius cydno* females and *Heliconius melpomene* males, F1
552 hybrid females are sterile, restricting us to a backcrossing design. We generated
553 backcross broods to *H. cydno* and *H. melpomene* by mating F1 males to virgin
554 females from our stock populations. Brood mothers were kept individually in cages
555 (approx. 1 or 2 x 2x2m), and provided with ~10% sugar solution, a source of pollen
556 and *Passiflora* shoots for oviposition. Eggs were collected daily and caterpillars
557 raised individually in small pots until 4th or 5th instar, and then either in groups or
558 individually until pupation. Caterpillars were provided with fresh *Passiflora* leaves and
559 shoots daily.
560
561 **Behavioral assays.** We measured male attraction to *H. melpomene* and *H. cydno*
562 females in standardized choice trials [25,38]. Males were allowed to mature for at
563 least 5 days after eclosion before testing. Males were introduced into outdoor
564 experimental cages (1x1x2m) with a virgin female of each species (0 – 10 days
565 matched for age). Fifteen-minute trials were divided into 1 min intervals, which were
566 scored for courtship (sustained hovering or chasing) directed towards each female as
567 having occurred or not occurred. Accordingly, if a male courted the same female
568 twice within a minute interval, it was recorded only once; if courtship continued into a
569 second minute, it was recorded twice. Where possible, trials were repeated for each
570 male (median = 5 trials). From these trials we generated a large dataset used in
571 subsequent analyses which includes the total number of 'courtship minutes' directed
572 towards *H. melpomene* and the number of 'courtship minutes' *H. cydno* females
573 (Table S2). The QTL analysis considered the proportion of total 'courtship minutes'
574 directed towards *H. melpomene, i.e.* 'courtship minutes' directed towards *H.*

575 *melpomene /* (‘courtship minutes’ directed towards *H. melpomene* + ‘courtship
576 minutes’ directed towards *H. cydno*) = “the relative amount of time males spent
577 courting red *H. melpomene* and white *H. cydno* females” = “relative courtship time”.
578 In total we conducted 1347 behavioral trials, and collected data from 28 *H. cydno*, 16
579 *H. melpomene*, 23 F1 hybrid, 29 backcross-to-*melpomene* hybrid and 196
580 backcross-to-*cydno* hybrid males (of which 11 performed no courtship behaviors).
581
582 **Genotyping and linkage map construction.** Genotyping and construction of
583 linkage maps has been described elsewhere [39]. In brief, backcross hybrids and
584 associated parents were preserved in 20% DMSO and 0.25M EDTA (pH 8.0) and
585 stored at -20°C. DNA was extracted with Qiagen DNeasy Blood & Tissue Kits
586 following the manufacture’s protocol for animal tissue. Individuals were genotyped
587 using a RAD-sequencing approach [69] and sequenced by BGI using the Illumina
588 HiSeq 2500. Sequences were then aligned to version 2 of the *H. melpomene*
589 genome [70] using Stampy v1.0.23 [71]. Duplicates were removed with Piccard tools
590 v1.135 (http://broadinstitute.github.io/picard/), and genotype posteriors called using
591 SAMtools v1.2. Interspecific linkage maps were constructed using Lep-MAP2 [72]
592 and modules from Lep-MAP3 as described in [39]. To obtain the genotypic data for
593 QTL mapping, the parental-phased data was obtained using Lep-MAP3
594 option outputPhasedData=1. This option imputes data based on input genotypes and
595 the map order. These data were then compared to the subset of markers in which
596 grandparents could be used to phase the data for each family and chromosome
597 using custom scripts. Family and chromosome was inverted when required to obtain
598 matching phases. Finally, the non-informative markers between inferred

599 recombinations were masked (i.e. set to missing) to account for the fact the exact
600 recombination position was not known for these regions.
601
602 **Data analysis.** All QTL analyses were performed on backcross-to-*cydno* hybrid
603 males in which the preference behaviors segregate. We were able to generate
604 genotype data for 146 of the 196 backcross-to-*cydno* hybrid males for which we
605 recorded behaviors in our choice trials. The remaining 50 individuals include males
606 from which we were unable to extract sufficient DNA, were poorly sequenced, or
607 were lost in the insectaries most often due to ants or other predators. For each
608 backcross individual, we calculated the probabilities of the two alternative genotypes
609 at every marker and centiMorgan (cM) position along the chromosomes, conditional
610 on the available marker data, using R/qtl package [73]. R/qtl uses a hidden Markov
611 model to calculate the probabilities of the true underlying genotypes given the
612 observed multipoint marker data. We then tested for an association between
613 phenotype and genotype at each position using generalized linear mixed models
614 (GLMMs) with binomial error structure and logit link function (implemented with the R
615 package lme4). We first considered the relative time males courted *H. melpomene* as
616 opposed to *H. cydno* females. For each position along the genome we modeled the
617 response vector of the number of 'courtship minutes' towards *H. melpomene* vs
618 'courtship minutes' towards *H. cydno* with the genotype probability as the
619 independent variable. LOD scores were obtained by comparing this to a null model in
620 which genotype probability was not included. An individual level random factor was
621 included in all models to account for over-dispersion. This approach is analogous to
622 the to the Haley-Knott regression implemented in R/qtl [54, 55], but more
623 appropriately accounts for the non-normal structure of our data and for differences in

624 total courtship data recorded for each individual [56]. Seven individuals were
625 excluded from these analyses for which, although tested in multiple trials, no
626 courtship towards either female type was recorded. Using permutation [57], we
627 determined the genome-wide significance threshold for the association between
628 marker genotype and phenotype (alpha = 0.05, n = 1000 permutations) as LOD =
629 2.99. By using our GLMM approach we had more power to detect QTL than would be
630 permitted by adopting non-parametric methods. Nevertheless, we repeated all QTL
631 analyses using non-parametric interval mapping in R/qtl, using the 'scanone' and
632 'model = "np" ' commands. Results of non-parametric analyses are reported in the
633 supplementary materials (Table S2).

634 To consider all three QTL identified in our initial genome scans together, we
635 again modeled the number of 'courtship minutes' towards *H. melpomene* vs
636 'courtship minutes' towards *H. cydno* but with the genotype at the max LOD score for
637 each QTL as explanatory variables. The fully saturated GLMM, including all three
638 pairwise interactions, was simplified in a stepwise manner using likelihood ratio tests,
639 but always retaining individual id as a random factor. To further test for effects of
640 each QTL we compared the penalized LOD scores of the full model (including all
641 three QTL as additive effects) to reduced models in which each QTL was eliminated
642 in turn. The penalized LOD score is calculated as: $pLODa(\gamma) = LOD(\gamma) - T|\gamma|$, where
643 γ denotes a model, $|\gamma|$ is the number of QTL in the model and T is a penalty
644 determined through permutation (i.e. the genome-wide significance threshold = 2.99)
645 [58] .

646 Finally, to determine the contribution of each QTL to variation in courtship time
647 towards *H. cydno* and *H. melpomene* females separately, we considered the total
648 number of 'courtship minutes' directed to each female type, correcting for the number

649 of trials. We included all 146 backcross males for which we had genotype data in this
650 analysis. We square-root transformed courtship minutes/trial and then used the
651 makeqtl() and fitqtl() functions in R/qtl [54] to determine significance. Model residuals
652 were inspected visually for an approximate normal distribution, and we tested for
653 homogeneity of variance with Levene's tests (*H. cydno* females: $F_{3,142} = 0.27$, $P > 0.02$;
654 *H. melpomene* females: $F_{3,142} = 0.39$, $P > 0.02$). We corrected *P* values to
655 account for the 6 tests (i.e. 3 loci x 2 species) [37].
656
657 **Simulations**. We used simulations to estimate potential inflation of measured effect
658 sizes due to the Beavis effect. We generated 10000 simulated data-sets for each of a
659 range of 'true' effect sizes for each significant QTL (i.e. on chromosomes 1, 17 and
660 18), using the R package simr [74]. For each of these we determined the LOD score
661 and compared it to our genome-wide significance threshold (i.e. LOD = 2.99). This
662 allowed us to compare i) the entire range of simulated effects (where the mean is
663 expected to equal the 'true' effect size), with those that would be significant given our
664 sample size (n = 139) and linkage map (figure S1), and ii) the empirically measured
665 effects with simulated effects that would be significant (Fig. 3A).
666
667 **Admixture analysis.** We investigated heterogeneity in admixture across the genome
668 between *H. melpomene rosina* and *H. cydno chioneus* using f_d, which provides an
669 approximately unbiased estimate of the admixture proportion [41,42]. This analysis
670 made use of available whole genome sequence data for *H. melpomene rosina*
671 (N=10) and *H. cydno chioneus* (N=10) from Panama, with *H. melpomene*
672 *melpomene* from French Guiana (N=10) serving as the allopatric 'control' population
673 and two *Heliconius numata* individuals as outgroups [42].

References

1. Nosil P. Ecological Speciation. Oxford University Press; 2012.

2. Gavrilets S. Fitness Landscapes and the Origin of Species. Princeton University Press; 2018.

3. Smadja CM, Butlin RK. A framework for comparing processes of speciation in the presence of gene flow. Mol Ecol. 2011;20: 5123–5140. doi:10.1111/j.1365-294X.2011.05350.x

4. Butlin RK, Smadja CM. Coupling, Reinforcement, and Speciation. Am Nat. 2018;191: 155–172. doi:10.1086/695136

5. Kopp M, Servedio MR, Mendelson TC, Safran RJ, Rodríguez RL, Hauber ME, et al. Mechanisms of Assortative Mating in Speciation with Gene Flow: Connecting Theory and Empirical Research. Am Nat. 2018;191: 1–20. doi:10.1086/694889

6. Servedio MR, Van Doorn GS, Kopp M, Frame AM, Nosil P. Magic traits in speciation: “magic” but not rare? Trends Ecol Evol (Amst). 2011;26: 389–397. doi:10.1016/j.tree.2011.04.005

7. Thibert-Plante X, Gavrilets S. Evolution of mate choice and the so-called magic traits in ecological speciation. Ecol Lett. 2013;16: 1004–1013. doi:10.1111/ele.12131

8. Lamichhaney S, Berglund J, Almén MS, Maqbool K, Grabherr M, Martinez-Barrio A, et al. Evolution of Darwin’s finches and their beaks revealed by genome sequencing. Nature. 2015;518: 371–375. doi:10.1038/nature14181

9. Albert AYK, Sawaya S, Vines TH, Knecht AK, Miller CT, Summers BR, et al. The genetics of adaptive shape shift in stickleback: pleiotropy and effect size. Evolution. 2008;62: 76–85. doi:10.1111/j.1558-5646.2007.00259.x

10. Arnegard ME, McGee MD, Matthews B, Marchinko KB, Conte GL, Kabir S, et al. Genetics of ecological divergence during speciation. Nature. 2014;511: 307–311. doi:10.1038/nature13301

11. Chung H, Loehlin DW, Dufour HD, Vaccarro K, Millar JG, Carroll SB. A single gene affects both ecological divergence and mate choice in Drosophila. Science. 2014;343: 1148–1151. doi:10.1126/science.1249998

12. Reed RD, Papa R, Martin A, Hines HM, Counterman BA, Pardo-Diaz C, et al. optix drives the repeated convergent evolution of butterfly wing pattern mimicry. Science. 2011;333: 1137–1141. doi:10.1126/science.1208227

13. Martin A, Papa R, Nadeau NJ, Hill RI, Counterman BA, Halder G, et al. Diversification of complex butterfly wing patterns by repeated regulatory evolution of a Wnt ligand. Proc Natl Acad Sci USA. 2012;109: 12632–12637. doi:10.1073/pnas.1204800109

14. Nadeau NJ, Pardo-Diaz C, Whibley A, Supple MA, Saenko SV, Wallbank RWR, et al. The gene cortex controls mimicry and crypsis in butterflies and moths. Nature. 2016;534: 106–110. doi:10.1038/nature17961

713 15. Bay RA, Arnegard ME, Conte GL, Best J, Bedford NL, McCann SR, et al. Genetic
714 Coupling of Female Mate Choice with Polygenic Ecological Divergence Facilitates
715 Stickleback Speciation. Curr Biol. 2017;27: 3344-3349.e4.
716 doi:10.1016/j.cub.2017.09.037

717 16. Lewontin RC, Kojima K. The Evolutionary Dynamics of Complex Polymorphisms.
718 Evolution. 1960;14: 458–472. doi:10.2307/2405995

719 17. Nosil P, Harmon LJ, Seehausen O. Ecological explanations for (incomplete) speciation.
720 Trends Ecol Evol. 2009;24: 145–156. doi:10.1016/j.tree.2008.10.011

721 18. Servedio MR, Noor MAF. The Role of Reinforcement in Speciation: Theory and Data.
722 Annual Review of Ecology, Evolution, and Systematics. 2003;34: 339–364.
723 doi:10.1146/annurev.ecolsys.34.011802.132412

724 19. Felsenstein J. Skepticism towards Santa Rosalia, or why are there so few kinds of
725 animals? Evolution. 1981;35: 124–138. doi:10.1111/j.1558-5646.1981.tb04864.x

726 20. Estrada C, Jiggins CD. Patterns of pollen feeding and habitat preference among
727 Heliconius species. Ecological Entomology. 2002;27: 448–456. doi:10.1046/j.1365-
728 2311.2002.00434.x

729 21. Jiggins CD, Naisbit RE, Coe RL, Mallet J. Reproductive isolation caused by colour
730 pattern mimicry. Nature. 2001;411: 302–305. doi:10.1038/35077075

731 22. Naisbit RE, Jiggins CD, Mallet J. Disruptive sexual selection against hybrids contributes
732 to speciation between Heliconius cydno and Heliconius melpomene. Proc Biol Sci.
733 2001;268: 1849–1854. doi:10.1098/rspb.2001.1753

734 23. Mavárez J, Salazar CA, Bermingham E, Salcedo C, Jiggins CD, Linares M. Speciation
735 by hybridization in Heliconius butterflies. Nature. 2006;441: 868–871.
736 doi:10.1038/nature04738

737 24. Merrill RM, Wallbank RWR, Bull V, Salazar PCA, Mallet J, Stevens M, et al. Disruptive
738 ecological selection on a mating cue. Proc Biol Sci. 2012;279: 4907–4913.
739 doi:10.1098/rspb.2012.1968

740 25. Merrill RM, Van Schooten B, Scott JA, Jiggins CD. Pervasive genetic associations
741 between traits causing reproductive isolation in Heliconius butterflies. Proc Biol Sci.
742 2011;278: 511–518. doi:10.1098/rspb.2010.1493

743 26. Merrill RM, Dasmahapatra KK, Davey JW, Dell'Aglio DD, Hanly JJ, Huber B, et al. The
744 diversification of Heliconius butterflies: what have we learned in 150 years? J Evol Biol.
745 2015;28: 1417–1438. doi:10.1111/jeb.12672

746 27. Southcott L, Kronforst MR. Female mate choice is a reproductive isolating barrier in
747 Heliconius butterflies | bioRxiv [Internet]. [cited 3 Aug 2018]. Available:
748 https://www.biorxiv.org/content/early/2017/12/12/233270

749 28. Jiggins CD. Ecological Speciation in Mimetic Butterflies. BioScience. 2008;58: 541–548.
750 doi:10.1641/B580610

751 29. Coyne JA, Orr HA. Speciation. Sinauer; 2004.

752 30. Montgomery SH, Merrill RM, Ott SR. Brain composition in Heliconius butterflies,
753 posteclosion growth and experience-dependent neuropil plasticity. J Comp Neurol.
754 2016;524: 1747–1769. doi:10.1002/cne.23993

755 31. Naisbit RE, Jiggins CD, Mallet J. Mimicry: developmental genes that contribute to
756 speciation. Evol Dev. 2003;5: 269–280.

757 32. Wallbank RWR, Baxter SW, Pardo-Diaz C, Hanly JJ, Martin SH, Mallet J, et al.
758 Evolutionary Novelty in a Butterfly Wing Pattern through Enhancer Shuffling. PLoS Biol.
759 2016;14: e1002353. doi:10.1371/journal.pbio.1002353

760 33. Van Belleghem SM, Rastas P, Papanicolaou A, Martin SH, Arias CF, Supple MA, et al.
761 Complex modular architecture around a simple toolkit of wing pattern genes. Nat Ecol
762 Evol. 2017;1: 52. doi:10.1038/s41559-016-0052

763 34. Nosil P, Schluter D. The genes underlying the process of speciation. Trends Ecol Evol
764 (Amst). 2011;26: 160–167. doi:10.1016/j.tree.2011.01.001

765 35. Kronforst MR, Young LG, Kapan DD, McNeely C, O'Neill RJ, Gilbert LE. Linkage of
766 butterfly mate preference and wing color preference cue at the genomic location of
767 wingless. Proc Natl Acad Sci USA. 2006;103: 6575–6580.
768 doi:10.1073/pnas.0509685103

769 36. Chamberlain NL, Hill RI, Kapan DD, Gilbert LE, Kronforst MR. Polymorphic butterfly
770 reveals the missing link in ecological speciation. Science. 2009;326: 847–850.
771 doi:10.1126/science.1179141

772 37. Forstmeier W, Wagenmakers E-J, Parker TH. Detecting and avoiding likely false-
773 positive findings - a practical guide. Biol Rev Camb Philos Soc. 2017;92: 1941–1968.
774 doi:10.1111/brv.12315

775 38. Merrill RM, Gompert Z, Dembeck LM, Kronforst MR, McMillan WO, Jiggins CD. Mate
776 preference across the speciation continuum in a clade of mimetic butterflies. Evolution.
777 2011;65: 1489–1500. doi:10.1111/j.1558-5646.2010.01216.x

778 39. Davey JW, Barker SL, Rastas PM, Pinharanda A, Martin SH, Durbin R, et al. No
779 evidence for maintenance of a sympatric Heliconius species barrier by chromosomal
780 inversions. Evolution Letters. 2017;1: 138–154. doi:10.1002/evl3.12

781 40. Beavis WB. The power and deceit of QTL experiments: lessons from comparative QTL
782 studies. 1994 *In*: Wilkinson (ed) Chicago pp 250-266

783 41. Martin SH, Davey JW, Jiggins CD. Evaluating the use of ABBA-BABA statistics to
784 locate introgressed loci. Mol Biol Evol. 2015;32: 244–257. doi:10.1093/molbev/msu269

785 42. Martin SH, Davey J, Salazar C, Jiggins C. Recombination rate variation shapes barriers
786 to introgression across butterfly genomes. bioRxiv. 2018; 297531. doi:10.1101/297531

787 43. Fisher RA. The Genetical Theory of Natural Selection: A Complete Variorum Edition.
788 OUP Oxford; 1999.

789 44. Weber JN, Peterson BK, Hoekstra HE. Discrete genetic modules are responsible for
790 complex burrow evolution in Peromyscus mice. Nature. 2013;493: 402–405.
791 doi:10.1038/nature11816

45. Diao W, Mousset M, Horsburgh GJ, Vermeulen CJ, Johannes F, van de Zande L, et al. Quantitative Trait Locus Analysis of Mating Behavior and Male Sex Pheromones in Nasonia Wasps. G3 (Bethesda). 2016;6: 1549–1562. doi:10.1534/g3.116.029074

46. Seimiya M, Gehring WJ. The Drosophila homeobox gene optix is capable of inducing ectopic eyes by an eyeless-independent mechanism. Development. 2000;127: 1879–1886.

47. Martin A, McCulloch KJ, Patel NH, Briscoe AD, Gilbert LE, Reed RD. Multiple recent co-options of Optix associated with novel traits in adaptive butterfly wing radiations. Evodevo. 2014;5: 7. doi:10.1186/2041-9139-5-7

48. Maynard Smith J. Sympatric Speciation. The American Naturalist. 1966;100: 637–650.

49. Hawthorne DJ, Via S. Genetic linkage of ecological specialization and reproductive isolation in pea aphids. Nature. 2001;412: 904–907. doi:10.1038/35091062

50. Shaw KL, Lesnick SC. Genomic linkage of male song and female acoustic preference QTL underlying a rapid species radiation. Proc Natl Acad Sci USA. 2009;106: 9737–9742. doi:10.1073/pnas.0900229106

51. Wiley C, Shaw KL. Multiple genetic linkages between female preference and male signal in rapidly speciating Hawaiian crickets. Evolution. 2010;64: 2238–2245. doi:10.1111/j.1558-5646.2010.01007.x

52. Wiley C, Ellison CK, Shaw KL. Widespread genetic linkage of mating signals and preferences in the Hawaiian cricket Laupala. Proc Biol Sci. 2012;279: 1203–1209. doi:10.1098/rspb.2011.1740

53. McNiven VTK, Moehring AJ. Identification of genetically linked female preference and male trait. Evolution. 2013;67: 2155–2165. doi:10.1111/evo.12096

54. Pryke SR. Sex chromosome linkage of mate preference and color signal maintains assortative mating between interbreeding finch morphs. Evolution. 2010;64: 1301–1310. doi:10.1111/j.1558-5646.2009.00897.x

55. Saether SA, Saetre G-P, Borge T, Wiley C, Svedin N, Andersson G, et al. Sex chromosome-linked species recognition and evolution of reproductive isolation in flycatchers. Science. 2007;318: 95–97. doi:10.1126/science.1141506

56. Ortíz-Barrientos D, Noor MAF. Evidence for a One-Allele Assortative Mating Locus. Science. 2005;310: 1467–1467. doi:10.1126/science.1121260

57. Chouteau M, Llaurens V, Piron-Prunier F, Joron M. Polymorphism at a mimicry supergene maintained by opposing frequency-dependent selection pressures. PNAS. 2017; 201702482. doi:10.1073/pnas.1702482114

58. Darragh K, Vanjari S, Mann F, Gonzalez-Rojas MF, Morrison CR, Salazar C, et al. Male sex pheromone components in Heliconius butterflies released by the androconia affect female choice. PeerJ. 2017;5: e3953. doi:10.7717/peerj.3953

59. Naisbit RE, Jiggins CD, Linares M, Salazar C, Mallet J. Hybrid sterility, Haldane's rule and speciation in Heliconius cydno and H. melpomene. Genetics. 2002;161: 1517–1526.

832 60. Boggs CL. Selection pressures affecting male nutrient investment in mating in
833 Heliconiine butterflies. Evolution. 1981;35: 931–940. doi:10.1111/j.1558-
834 5646.1981.tb04959.x

835 61. Boggs CL, Gilbert LE. Male contribution to egg production in butterflies: evidence for
836 transfer of nutrients at mating. Science. 1979;206: 83–84.
837 doi:10.1126/science.206.4414.83

838 62. Kronforst MR, Young LG, Gilbert LE. Reinforcement of mate preference among
839 hybridizing Heliconius butterflies. J Evol Biol. 2007;20: 278–285. doi:10.1111/j.1420-
840 9101.2006.01198.x

841 63. Servedio MR. Beyond reinforcement: the evolution of premating isolation by direct
842 selection on preferences and postmating, prezygotic incompatibilities. Evolution.
843 2001;55: 1909–1920.

844 64. Jiggins CD, Estrada C, Rodrigues A. Mimicry and the evolution of premating isolation in
845 Heliconius melpomene Linnaeus. J Evol Biol. 2004;17: 680–691. doi:10.1111/j.1420-
846 9101.2004.00675.x

847 65. Walters JR, Stafford C, Hardcastle TJ, Jiggins CD. Evaluating female remating rates in
848 light of spermatophore degradation in Heliconius butterflies: pupal-mating monandry
849 versus adult-mating polyandry. Ecological Entomology. 2012;37: 257–268.
850 doi:10.1111/j.1365-2311.2012.01360.x

851 66. Seehausen O, Terai Y, Magalhaes IS, Carleton KL, Mrosso HDJ, Miyagi R, et al.
852 Speciation through sensory drive in cichlid fish. Nature. 2008;455: 620–626.
853 doi:10.1038/nature07285

854 67. Greenwood AK, Wark AR, Yoshida K, Peichel CL. Genetic and neural modularity
855 underlie the evolution of schooling behavior in threespine sticklebacks. Curr Biol.
856 2013;23: 1884–1888. doi:10.1016/j.cub.2013.07.058

857 68. Melo MC, Salazar C, Jiggins CD, Linares M. Assortative mating preferences among
858 hybrids offers a route to hybrid speciation. Evolution. 2009;63: 1660–1665.
859 doi:10.1111/j.1558-5646.2009.00633.x

860 69. Baird NA, Etter PD, Atwood TS, Currey MC, Shiver AL, Lewis ZA, et al. Rapid SNP
861 discovery and genetic mapping using sequenced RAD markers. PLoS ONE. 2008;3:
862 e3376. doi:10.1371/journal.pone.0003376

863 70. Davey JW, Chouteau M, Barker SL, Maroja L, Baxter SW, Simpson F, et al. Major
864 Improvements to the Heliconius melpomene Genome Assembly Used to Confirm 10
865 Chromosome Fusion Events in 6 Million Years of Butterfly Evolution. G3 (Bethesda).
866 2016;6: 695–708. doi:10.1534/g3.115.023655

867 71. Lunter G, Goodson M. Stampy: a statistical algorithm for sensitive and fast mapping of
868 Illumina sequence reads. Genome Res. 2011;21: 936–939. doi:10.1101/gr.111120.110

869 72. Rastas P, Paulin L, Hanski I, Lehtonen R, Auvinen P. Lep-MAP: fast and accurate
870 linkage map construction for large SNP datasets. Bioinformatics. 2013;29: 3128–3134.
871 doi:10.1093/bioinformatics/btt563

872 73. Broman KW, Wu H, Sen S, Churchill GA. R/qtl: QTL mapping in experimental crosses.
873 Bioinformatics. 2003;19: 889–890.

74. Green P, MacLeod CJ. SIMR: an R package for power analysis of generalized linear mixed models by simulation. Methods in Ecology and Evolution. 2016;7: 493–498. doi:10.1111/2041-210X.12504

Acknowledgements We are grateful to Moisés Abanto, Josephine Dessmann, Janet Scott and Bas van Schooten for help in the insectaries, to Justin Touchon for advice regarding statistics, and to Stephen Montgomery, Markus Möst, Ricardo Pereira, Alexander Hausmann and Vera Warmuth for comments on the manuscript. We are also grateful for insightful referee comments which greatly improved this manuscript. We thank the Smithsonian Tropical Research Institute for support and the Ministerio del Ambiente for permission to collect butterflies in Panama. We are also grateful to Edinburgh Genomics for sequencing support. RMM is funded by a DFG Emmy Noether Fellowship, and was also funded by a Junior Research Fellowship at King's College, Cambridge and by the ERC grant 339873 Speciation Genetics awarded to CJ. JD was funded by a Herchel Smith Postdoctoral Fellowship. SHM was funded by a research fellowship from St John's College, Cambridge.

Supporting Information

Figure S1. Overview of crossing design. Colored boxes represent segregating *H. cydno* (blue) and *H. melpomene* (orange) alleles; Z and W refer to the alleles on the sex-chromosomes and A to those on autosomes.

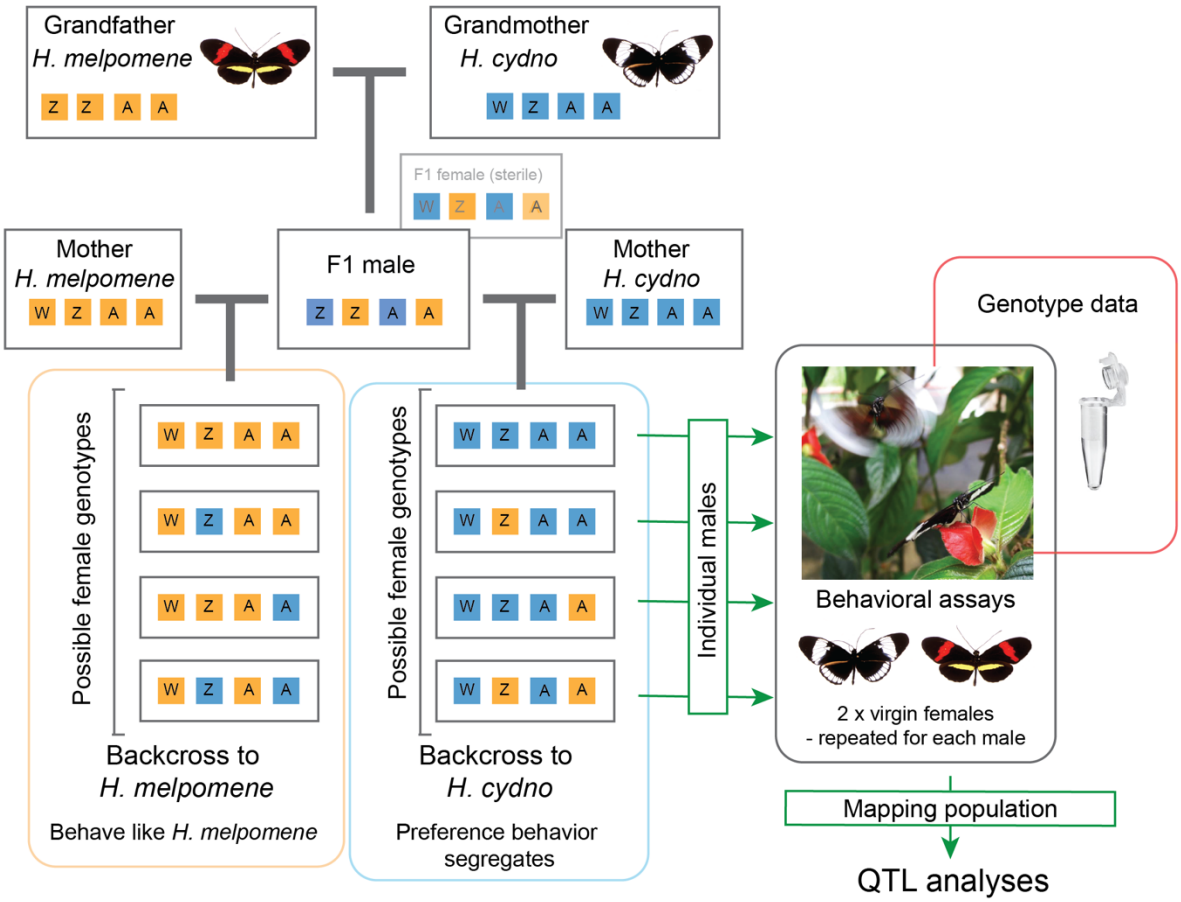

914 **Figure S2. QTL analysis of variation of mate preference for individuals with alternative**
915 **genotypes at LG18@0cM.** QTL associated with the proportion of time males court *H. melpomene* (as
916 opposed to *H. cydno*) females on chromosomes 17 for individuals homozygous (i.e. white, CYD:CYD
917 = blue line) and heterozygous (i.e. red, CYD:MEL = orange line) at LG18@0cM. Dashed line
918 represents log odds ratio (LOD) significance threshold (*i.e.* genome-wide alpha = 0.05) for
919 heterozygous (*i.e.* red, CYD:MEL) individuals. Dashes along the x-axis indicate position of genetic
920 markers (SNPs).

921

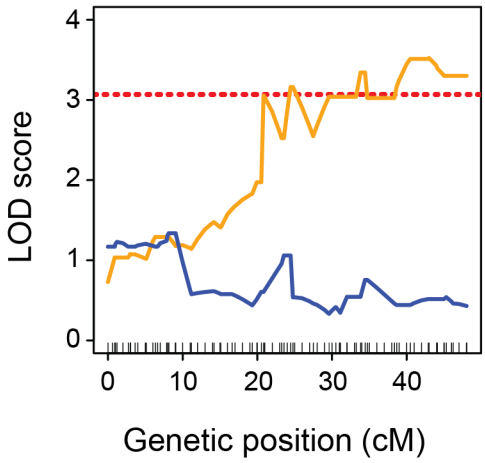

922

923

924

925

926

927

928

929

930

931

932

933

934 **Figure S3. Simulations suggest QTL effect sizes are not greatly overestimated.** For each
935 simulated effect size, the distribution of all simulated effects (blue) and those which would be
936 significant in our analysis (*i.e.* LOD ≥ 2.99) (orange) are shown. In each case, 'recorded' refers to the
937 empirically measure effect size.

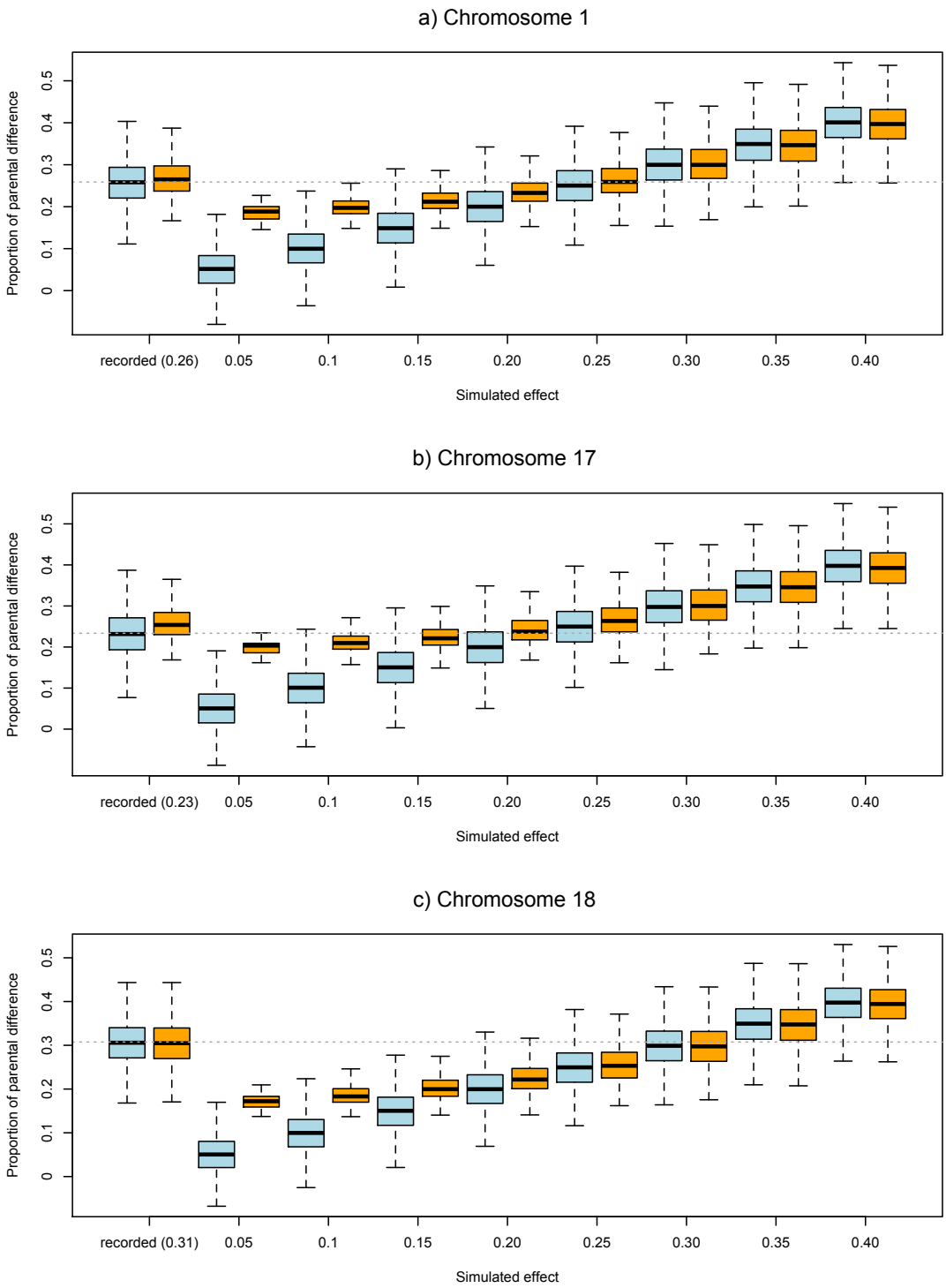

938

939

940 **Figure S5. Localized levels of admixture (f_d) across all 21 chromosomes.** Blue points represent f_d
941 values for 100kb windows. f_d was measured between *H. melpomene rosina* and *H. cydno chioneus*
942 individuals.
943

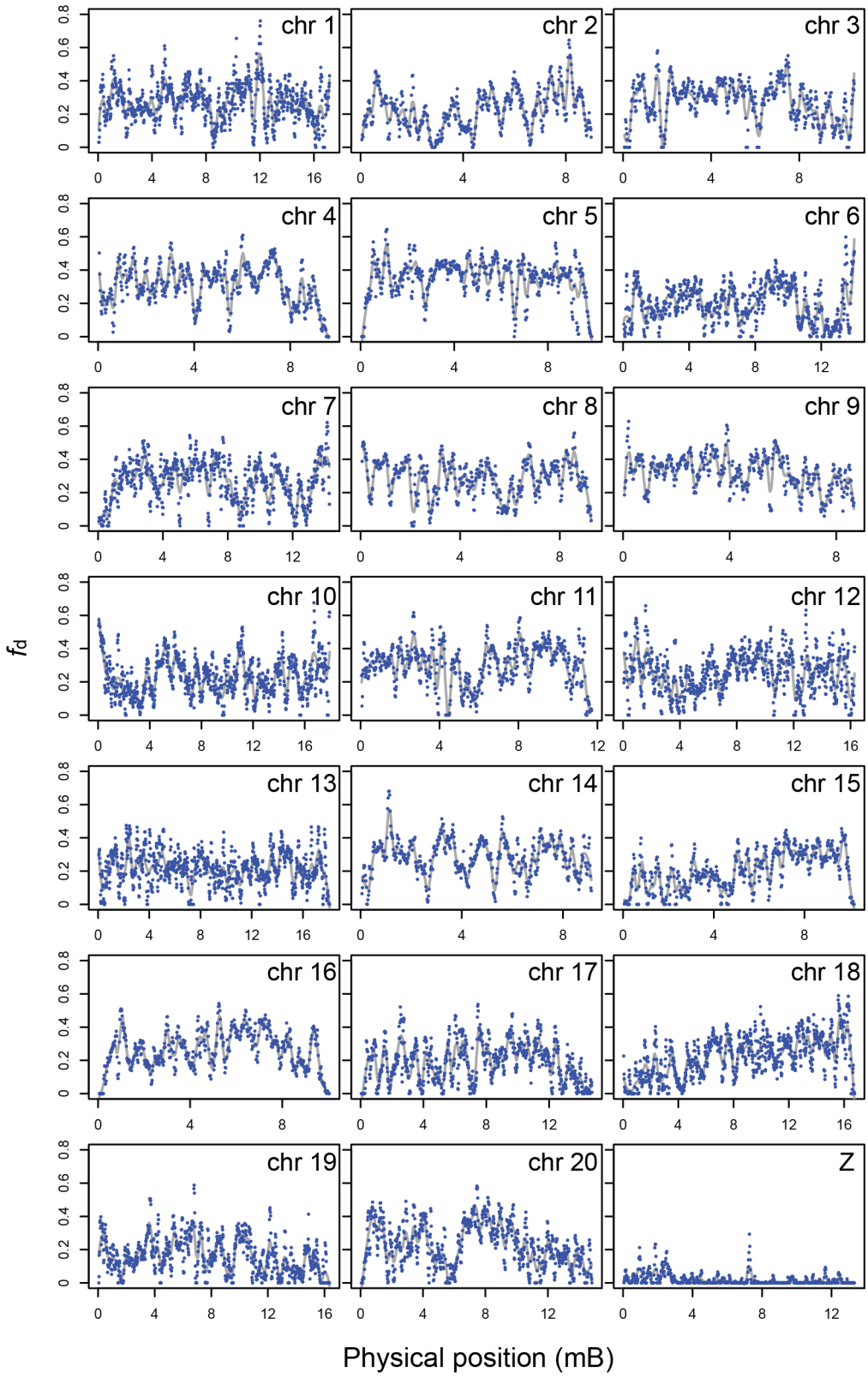

944

945 **Figure S5. Decline in linkage disequilibrium (LD) of linked and unlinked loci under an**
946 **assumption of random mating.** Whereas linkage disequilibrium (*D*) between unlinked loci (red solid
947 line) declines by 50% in one generation of random mating, LD between two loci that are 1.2cM apart
948 would decline by only 1.2 % per generation (black solid line), and LD between two loci that are 4.8cM
949 apart (gray dashed line) would decline by only 4.6% per generation.

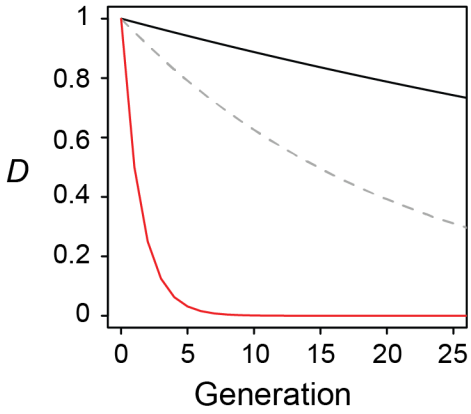

950

951

952

953 **Table S1. Summary of genome-wide QTL analyses using binomial GLMM methods (reported in**
954 **main text) and non-parametric methods implemented in R/qtl.**

	Binomial GLMM			**Non-parametric**		
Chromosome	Position (cM)	LOD	*P*	Position (cM)	LOD	*P*
1	4.23	4.54	<0.001	4.23	3.6	~0.009
17	24.47	3.5	~0.013	24.47	2.89	~0.049
18	0	6.83	<0.001	0	5.34	<0.001

955 Position in cM refers to the position the peak lod score, i.e. the most likely genetic position of the
956 putative QTL, for each QTL. *P* values are determined through permutation as described in the
957 methods.
958

959

960

961 **Table S2. Courtship data and total trials for all 292 individuals included in the study.** Type CYD
962 = pure *H. cydno chioneus*; MEL = pure *H. melpomene rosina*; F1 = first generation hybrids (*H. cydno*
963 *chioneus* mother and *H. melpomene rosina* father); BC = backcross to *H. cydno chioneus*; and BM =
964 backcross to *H. melpomene rosina.*
965
966 *See attached .csv file:* Table_S2.csv
967